U.S. DEPARTMENT OF THE INTERIOR
U.S. GEOLOGICAL SURVEY

IMAGING AND GROUND MOTION IN URBAN SEDIMENTARY BASINS: THE SANTA CLARA AND SAN BERNARDINO VALLEYS

by

Stephen Hartzell, Robert Jachens, Thomas Brocher, and Arthur Frankel

U.S. Geological Survey Open-File Report 98-244

Introduction

Following the 1994 Northridge earthquake in Los Angeles, California, and the 1995 Hyogo-ken Nanbu earthquake in Kobe, Japan, ground motion records became available that demonstrated the importance of deep basin structure for strong-ground motion and its correlation with observed damage patterns (Iwata *et al.*, 1996; Pitarka *et al.*, 1996; Kawase, 1996; Hartzell *et al.*, 1997; Wald and Graves, 1998; Graves *et al.*, 1998). The U.S. Geological Survey Earthquake Hazards Program Five Year Plan 1998-2002 (Page *et al.*, 1998) recognized the significant hazard and risk that earthquake ground motion in urban basins presents, and called for a workshop to choose an earthquake-prone urban basin as a focus for future investigations. On April 22, 1998 a workshop was held at the Menlo Park, California, office of the U.S. Geological Survey for the purpose of selecting an urban sedimentary basin to conduct 3D wave propagation and ground motion studies. That workshop chose the Santa Clara Valley as the primary study area and the San Bernardino Valley the secondary study area. These selections were later endorsed by the NEHRP Earthquake Program Council.

The purpose of this report is to give a brief review of our current knowledge of the structure of these two basins and the work that is needed to better understand the ground motion hazards that exist. Figures 1 and 2 show the probabilities of exceeding the current design criterion in a 30 year period for rock sites in the Santa Clara and San Bernardino Valleys, respectively (Frankel *et al.*, 1996). Effects of the sediment-filled basins are not considered. Both areas show a significant hazard, with San Bernardino being higher than

Santa Clara. The Santa Clara area, however, has a higher risk due to a greater population density and industrial development.

Basin Structure Information

Santa Clara

Brocher *et al.* (1997) have developed a detailed 3D velocity model for the entire San Francisco Bay area. The Santa Clara Valley is a section of this model. The data used to construct the model come from a variety of sources: geologic considerations, seismic reflection and refraction, gravity inversion, water wells, and drill-hole logs. The major units are: 1) mantle, 2) mafic lower crust 3) basement middle crust (Franciscan complex), 4) basement middle crust (Salinian plutonic and metamorphic), 5) Cretaceous and Tertiary sedimentary rocks, 6) Pliocene and Quaternary sediments. Within the basement and overlying units the model velocities are gradients. For the region of the Santa Clara Valley, the model includes a detailed surficial geologic classification as well. There is no topography in the model. Figures 3, 4, and 5 show the locations of water wells, USGS drill-holes, and refraction lines, respectively, that are available for the Santa Clara Valley, and have been used to construct the velocity model. The USGS drill-holes (Gibbs *et al.*, 1975; 1976; 1977; 1992) are logged for P- and S-wave velocities and have depths from 30 to 100m. Figure 6 shows the estimated depth to pre-Cenozoic basement (either Franciscan, coast range ophiolite, or Salinian granitic/metamorphic). Primary features are two deeper parts of the basin, the Cupertino Basin along the west edge of the valley and the Evergreen Basin along the east edge. The valley is bounded on the west by the San Andreas and

Monte Vista Faults and on the east by the Calaveras/Hayward fault system. How seismic waves from sources on these faults are affected by the sedimentary basin is a primary research objective.

A second velocity model of the area has been developed by Antolick *et al.* (1997) and Larsen *et al.* (1997). This model has been used to model the Loma Prieta earthquake (Antolick *et al.*, 1998) and scenario earthquakes on the Hayward Fault (Larsen *et al.*, 1998).

San Bernardino

Less structural information is available for the San Bernardino basin. What is known is based primarily on gravity data and a few wells that reach basement. Figure 7 shows the depth to pre-Cenozoic basement (Pelona Schist or San Bernardino Mtns. granitic/metamophic) based on gravity inversion. The San Bernardino Valley is bounded by the San Andreas Fault on the north side and the San Jacinto and Rialto-Colton Faults on the south side. Wells that reach basement are given in Table 1 (Dutcher and Garrett, 1963).

Table 1

San Bernardino Well Information

Latitude	Longitude	Depth to Basement (ft)
34.0735	-117.1375	390.
34.0705	-117.1287	210.
34.0816	-117.3469	1185.
34.1363	-117.2729	330.
34.0740	-117.1118	200.
34.0770	-117.0796	100.
34.0114	-117.2674	213.
34.0018	-117.0994	5358.
34.0576	-117.1658	213.
34.0646	-117.1400	470.
34.0583	-117.1253	250.
34.0953	-117.3959	371.

Table 2

Rialto-Colton 1000 ft Sonic Logs

Latitude	Longitude
34.0914	-117.2349
34.0800	-117.2359
34.0606	-117.2238
34.0804	-117.2216
34.0559	-117.1945

One refraction line was done in the San Bernardino Valley by Hadley and Combs (1974) along the Santa Ana River channel. However, their interpretation of this refraction line is inconsistent with the gravity inversion in Figure 7. Both show the deepest part of the basin to be at its southwestern edge near the merging of the San Jacinto and Rialto-Colton Faults. Gravity, however, shows a rapidly shallowing basin to the northeast and the refraction line suggests the basin remains deep.

In addition, six 1000 ft holes have been drilled in the Rialto-Colton basin and sonic logs obtained (Table 2) (Linda Woolfenden, personal commmunication, 1998). The Rialto-Colton basin lies just to the west of the San Bernardino Valley (Figure 7). Water wells have also been used to infer geologic cross sections through the San Bernardino Valley basin by Izbicki *et al.* (1997) and Danskin *et al.* (1998). Initial shallow P- and S-wave velocity measurements have been taken in the San Bernardino Valley using the seismic refraction method of Williams *et al.* (1997). These velocity profiles are judged to be accurate to a depth of 30m. Figure 8 shows the sites where these measurements have been made.

Ground Motion Availability

Earthquake ground motion recordings are needed to test modeling codes, validate predictions of ground motion, and update our knowledge of the 3D velocity structures.

Santa Clara

Figure 9 shows the strong-ground motion stations that recorded data for three recent earthquakes: 1989, M_w6.9 Loma Prieta; 1984, M_L6.2 Morgan Hill; and 1979, M_L 5.8 Coyote Lake. In addition to these mainshock records, the Loma Prieta earthquake provided a significant number of aftershock records in the Santa Clara Valley. Figure 10 shows the aftershock station locations (Mueller and Glassmoyer, 1990) in and near the valley. The data from many of these stations have been used to estimate local site response (Boatwright *et al.*, 1991; Fletcher and Boatwright, 1991; Hartzell, 1992). A dense array in Sunnyvale also recorded several aftershocks and was used to study basin surface waves (Frankel *et al.*, 1991).

Three-dimensional wave propagation modeling in the Santa Clara Valley is limited. Frankel and Vidale (1992), used a simple two-component velocity model (sediment and bedrock) based on water wells to propagate elastic waves through the valley for a magnitude 4.4 aftershock of Loma Prieta. Recently, Antolik *et al.* (1998) have done a 3D numerical simulation of the Loma Prieta mainshock using a more elaborate velocity model.

San Bernardino

Figure 11 shows the location of strong motion instruments in the San Bernardino Valley. These stations recorded the 1992, M_w 7.2 Landers earthquake and the 1991, M_w 5.6 Sierra Madre earthquake among other smaller events. In addition, there is a recently completed 100m deep drill-hole at the San Bernardino Central Fire Station (34.1052, -117.2798) (Rogers *et al.*, 1998). This hole is instrumented with both surface and down-hole broadband seismometers. Also, many aftershocks of the Landers and Big Bear earthquakes were recorded on three dense arrays deployed in the San Bernardino Valley (Frankel, 1994).

Three-dimensional waveform modeling in the San Bernardino Valley is more limited than in the Santa Clara Valley. Studies by Frankel (1993; 1994) used alluvium and basement units and a depth to basement based on limited well information.

Future Work

Imaging

The relevant properties of alluvial basins must be well specified before their seismic responses can be accurately calculated. The properties include: 1) the geometry of the basin (the shape of the sediment/basement interface as well as structures within the sedimentary column), 2) the velocity structure, 3) attenuation, and 4) the location and orientation of significant faults. In other words, spatial seismic velocity changes are of particular interest, whether at the basement interface or within the basin itself, that produce a significant modification of the wavefield. The most efficient and direct means of acquiring this information is by active-source seismic reflection/refraction profiles. These experiments should be designed to maximize resolution in the upper 5 km of the crust or to the depth of the pre-Cenozoic basement. Both the Santa Clara and San Bernardino Valleys have very little data of this type. Consideration needs to be given to what field procedure is best to accomplish this goal, that is, reflection versus refraction, Vibroseis source versus explosion source, etc.

Inversion of gravity and magnetic data have also proved useful in defining basin geometry as well as the dip on faults. Langenheim *et al.* (1997) modeled gravity and aeromagnetic data to help constrain the dip of the Monte Vista Fault on the western margin of the Santa Clara Valley. Efforts should be made to see that all available well information is included in these inversions to help constrain the solution.

In addition, shallow imaging of the top 30 to 100m is needed to accurately determine P- and S-wave velocities. These profiles are needed to calculate the local site response caused by shallow velocity variations and to distinguish shallow from deeper effects.

A typical finite-difference calculation to an upper frequency of 1 Hz may require a grid spacing of approximately 100m with physical properties specified at this interval. Resolution of large urban basins in 3D at this scale is not a practical objective. The key to productive research will be the discovery of those structures that contribute most significantly to the observed ground motion, such as structures causing focusing or basin edge effects (Gao *et al.*, 1996; Hartzell *et al.*, 1997; Graves *et al.*, 1998), and to image them as well as possible.

Ground Motion

Ground motion measurements are vital for observing the response of an alluvial basin and for checking model predictions. At present, ground motion instrumentation in both the Santa Clara and San Bernardino Valleys is limited to a few widely spaced strong motion instruments. For the Santa Clara Valley there are a few additional aftershock recordings of the Loma Prieta earthquake. Data from many more free-field recording sites are needed with a spacing of approximately 1 km. The close spacing is required to resolve spatial differences caused by subsurface structures that have been observed in other sedimentary basins (Hartzell *et al.*, 1997). These instruments should be designed to record weak motions as well as strong motions to enable the recording of background seismicity ($M_L 3.0$). This flexibility will allow the instruments to be moved to new locations fairly frequently.

Modeling

The accuracy of 3D wave propagation codes needs to be checked by comparing the results of different algorithms. Existing 3D velocity models should be used to simulate both aftershock and mainshock data records to determine the weaknesses of these models. The velocity models can then be modified to produce better comparisons with the data.

These new models need to incorporate and be checked against new basin imaging data as it becomes available.

Improvements in 3D wave propagation codes are needed to make large problems more efficient and practical. Variable grid sizing would reduce the size of the problems by using larger grid spacing for regions with higher seismic velocities. Other improvements would include models with topography and codes designed to take advantage of multi-processor CPUs.

Acknowledgements

This report was significantly improved by the contribution of figures and information by several individuals: David Boore, Wes Danskin, Jim Gibbs, Vicki Langenheim, Doug Morton, Chuck Mueller, Paul Spudich, David Wald, Carl Wentworth, and Linda Woolfenden. The clarity of the report was improved by reviewers Rob Wesson and Rus Wheeler.

References

Antolik, M., Stidham, C., Dreger, D., Larsen, S., Lomax ,A., and Romanowicz, B. (1997), 2-D and 3-D models of broadband wave propagation in the San Francisco Bay region and north coast ranges: Seism. Res. Lett., v. 68, p. 328.

Antolik, M., Dreger, D., Stidham, C., Romanowicz, B., and Larsen, S. (1998), Three-Dimensional numerical simulation of the seismic wavefield of the 1989 Loma Prieta earthquake: Science, submitted.

Boatwright, J., Fletcher, J., and Fumal, T. (1991), A general inversion scheme for source, site, and propagation characteristics using multiply recorded sets of moderate-sized earthquakes: Bull. Seism. Soc. Am., v. 81, p. 1754-1782.

Brocher, T., Brabb, E., Catchings, R., Fuis, G., Fumal, T., Jachens, R., Jayko, A., Kayen, R., McLaughlin, R., Parsons, T., Rymer, M., Stanley, R., Wentworth, C. (1997), A crustal-scale 3-D seismic velocity model for the San Francisco Bay area, California: EOS, Trans. Amer. Geophys. Un., Supplement, v. 78, no. 46, p. F435-F436.

Danskin, W., Woolfenden, L., and McPherson, K. (1998), Hydrology, description of computer models, and evaluation of selected water-management alternatives in the San Bernardino area, California: U.S. Geological Survey Open-File Report 98-XXX.

Dutcher, L., Garret, A. (1963), Geologic and hydrologic features of the San Bernardino area, California: U.S. Geological Survey water-supply paper 1419, 114 p.

Fletcher, J., and Boatwright, J. (1991), Source parameters of Loma Prieta aftershocks and wave propagation characteristics along the San Francisco Peninsula from a joint inversion of digital seismograms: Bull. Seism. Soc. Am., v. 81, p. 1783-1812.

Frankel, A. (1993), Three-dimensional simulations of ground motions in the San Bernardino Valley, California, for hypothetical earthquakes on the San Andreas Fault: Bull. Seism. Soc. Am., v. 83, p. 1020-1041.

Frankel, A. (1994), Dense array recordings in the San Bernardino Valley of Landers-Big Bear aftershocks: Basin surface waves, Moho reflections, and three-dimensional simulations: Bull. Seism. Soc. Am., v. 84, p. 613-624.

Frankel, A., Hough, S., Friberg, P., and Busby, R. (1991), Observations of Loma Prieta aftershocks from a dense array in Sunnyvale, California: Bull. Seism. Soc. Am., v. 81, p. 1900-1922.

Frankel, A., and Vidale, J. (1992), A three-dimensional simulation of seismic waves in the Santa Clara Valley, California, from a Loma Prieta aftershock: Bull. Seism. Soc. Am., v. 82, p. 2045-2074.

Frankel, A., Mueller, C., Barnhard, T., Perkins, D., Leyendecker, E.V., Dickman, N., Hanson, S., and Hopper, M. (1996), National seismic-hazard maps: Documentation June 1996: U.S. Geological Survey Open-File Report 96-532, 110 p.

Gao, S., Liu, H., Davis, P. M., and Knopoff, L. (1996), Localized amplification of seismic waves and correlation with damage due to the Northridge earthquake: evidence for focusing in Santa Monica: Bull. Seism. Soc. Am., v. 86, p. S209-S230.

Gibbs, J., Fumal, T., and Borcherdt, R. (1975), In-situ measurements of seismic velocities at twelve locations in the San Francisco Bay region: U.S. Geological Survey Open-File Report 75-564, 87 p.

Gibbs, J., Fumal, T., and Borcherdt, R. (1976), In-situ measurements of seismic velocities in the San Francisco Bay region-Part II: U.S. Geological Survey Open-File Report 76-731, 145 p.

Gibbs, J., Fumal, T., Borcherdt, R., and Roth, E. (1977), In-situ measurements of seismic velocities in the San Francisco Bay region-Part III: U.S. Geological Survey Open-File Report 77-850, 143 p.

Gibbs, J., Fumal, T., Boore, D., and Joyner, W. (1992), Seismic velocities and geologic logs from borehole measurements at seven strong-motion stations that recorded the Loma Prieta earthquake: U.S. Geological Survey Open-File Report 92-287, 139 p.

Graves, R., Pitarka, A., and Somerville, P. (1998), Ground motion amplification in the Santa Monica area: Effects of shallow basin edge structure: Bull. Seism. Soc. Am., submitted.

Hadley, D., and Combs, J. (1974), Microearthquake distribution and mechanisms of faulting in the Fontana-San Bernardino area of southern California: Bull. Seism. Soc. Am., v. 64, p. 1477-1500.

Hartzell, S. (1992), Site response estimation from earthquake data: Bull. Seism. Soc. Am., v. 82, p. 2308-2327.

Hartzell, S., Cranswick, E., Frankel, A., Carver, D., and Meremonte, M. (1997), Variability of site response in the Los Angeles urban area: Bull. Seism. Soc. Am., v. 87, p. 1377-1400.

Iwata, T., Hatayama, K., Kawase, H., and Irikura, K. (1996), Site amplification of ground motions during aftershocks of the 1995 Hyogo-ken Nanbu earthquake in severely damaged zone–Array observation of ground motions in Higashinada Ward, Kobe City, Japan: J. Phys. Earth, v. 44, p. 553-561.

Izbicki, J., Danskin, W., and Mendez, G. (1997), Chemistry and isotopic composition of ground water along a section near the Newmark area, San Bernardino County, California: U.S. Geological Survey Water-Resources Investigations Report 97-4179.

Kawase, H. (1996), The cause of the damage belt in Kobe: "The basin-edge effect", constructive interference of the direct S-wave with the basin-induced diffracted/Raleigh waves: Seism. Res. Lett., v. 67, p. 25-34.

Langenheim, V., Schmidt, K., and Jachens, R. (1997), Coseismic deformation during the 1989 Loma Prieta earthquake and range-front thrusting along the southwestern margin of the Santa Clara Valley, California: Geology, v. 25, p. 1091-1094.

Larsen, S., Antolik, M., Dreger, D., Stidham, C., Schultz, C., Lomax, A., and Romanowicz, B. (1997), 3-D models of seismic wave propagation: Simulating scenario earthquakes along the Hayward Fault: Seism. Res. Lett., v. 68, p. 328.

Larsen, S., Antolik, M., Dreger, D., Stidham, C., Schultz, C., Lomax, A., and Romanowicz, B. (1998), 3-D simulations of scenario earthquakes along the Hayward Fault: in preparation.

Mueller, C., and Glassmoyer, G. (1990), Digital recordings of aftershocks of the 17 October 1989 Loma Prieta, California, earthquake: U.S. Geological Survey Open-File Report 90-503, 147 p.

Page, R.A., Mori, J., Roeloffs, E.A., and Schweig, E.S. (1998), Earthquake hazards program five year plan 1998-2002: U.S. Geological Survey Open-File Report 98-143, 37 p.

Pitarka, A., Irikura, K., Iwata, T., and Kagawa, T. (1996), Basin structure effects in the Kobe area inferred from the modeling of ground motions from two aftershocks of the January 17, 1995, Hyogo-ken Nanbu earthquake: J. Phys. Earth, v. 44, p. 563-576.

Rogers, A., Mueller, C., Tinsley, J., Gibbs, J., and Koesterer, C. (1998), Instrumentation of two vertical strong-motion arrays at Cerritos College, Norwalk and downtown San Bernardino, California: U.S. Geological Survey Open-File Report 98-XXX.

Wald, D., Graves, R. (1998), The seismic response of the Los Angeles basin, California: Bull. Seism. Soc. Am., v. 88, p. 337-356.

Williams, R., Stephenson, W., Odum, J., and Worley, D. (1997), High-resolution surface-seismic imaging techniques for NEHRP soil profile classifications and earthquake hazard assessments in urban areas: U.S. Geological Survey Open-File Report 97-501, 42 p.

Figure Captions

Figure 1. Contours of probability of exceeding the design criterion (0.4g) in a 30 year period for the Santa Clara Valley. The estimates are for rock sites.

Figure 2. Contours of probability of exceeding the design criterion (0.4g) in a 30 year period for the San Bernardino Valley. The estimates are for rock sites.

Figure 3. Distribution of water wells in and around the Santa Clara Valley used in the construction of the three-dimensional velocity model of the area. (Brocher *et al.*, 1997).

Figure 4. Distribution of drill-holes, logged for P- and S-wave velocity, with depths of 30 to 100m used to construct the three-dimensional velocity model of the area. (Brocher *et al.*, 1997).

Figure 5. Shot points (large solid circles) and receiver locations (small open circles) for seismic surveys in and around the Santa Clara Valley used to constrain the three-dimensional velocity model of the area. (Brocher *et al.*, 1997)

Figure 6. Depth to pre-Cenozoic basement for the Santa Clara Valley taken from the three-dimensional velocity model of the area (Brocher *et al.*, 1997). Small open squares are gravity stations on basement outcrop. Small open triangles are wells and seismic control on depth to basement.

Figure 7. Depth to pre-Cenozoic basement for the San Bernardino Valley from inversion of gravity measurements (Jachens, unpublished).

Figure 8. Sites with shallow P and S-wave velocity measurements to a depth of 30m base on seismic refraction (solid triangles). Pilot 650m long refraction line to map shape of alluvium/bedrock contact (solid square) (Robert Williams, personal communication, 1998).

Figure 9. Distribution of triggered strong-ground motion instruments in and around the Santa Clara Valley for recent earthquakes.

Figure 10. Distribution of aftershock recorders for the Loma Prieta earthquake in and around the Santa Clara Valley. (Mueller and Glassmoyer, 1990).

Figure 11. Distribution of strong-ground motion instruments in the San Bernardino Valley. Solid triangles (USGS), open triangles (CDMG), gray triangle on San Andreas Fault (TerraScope).

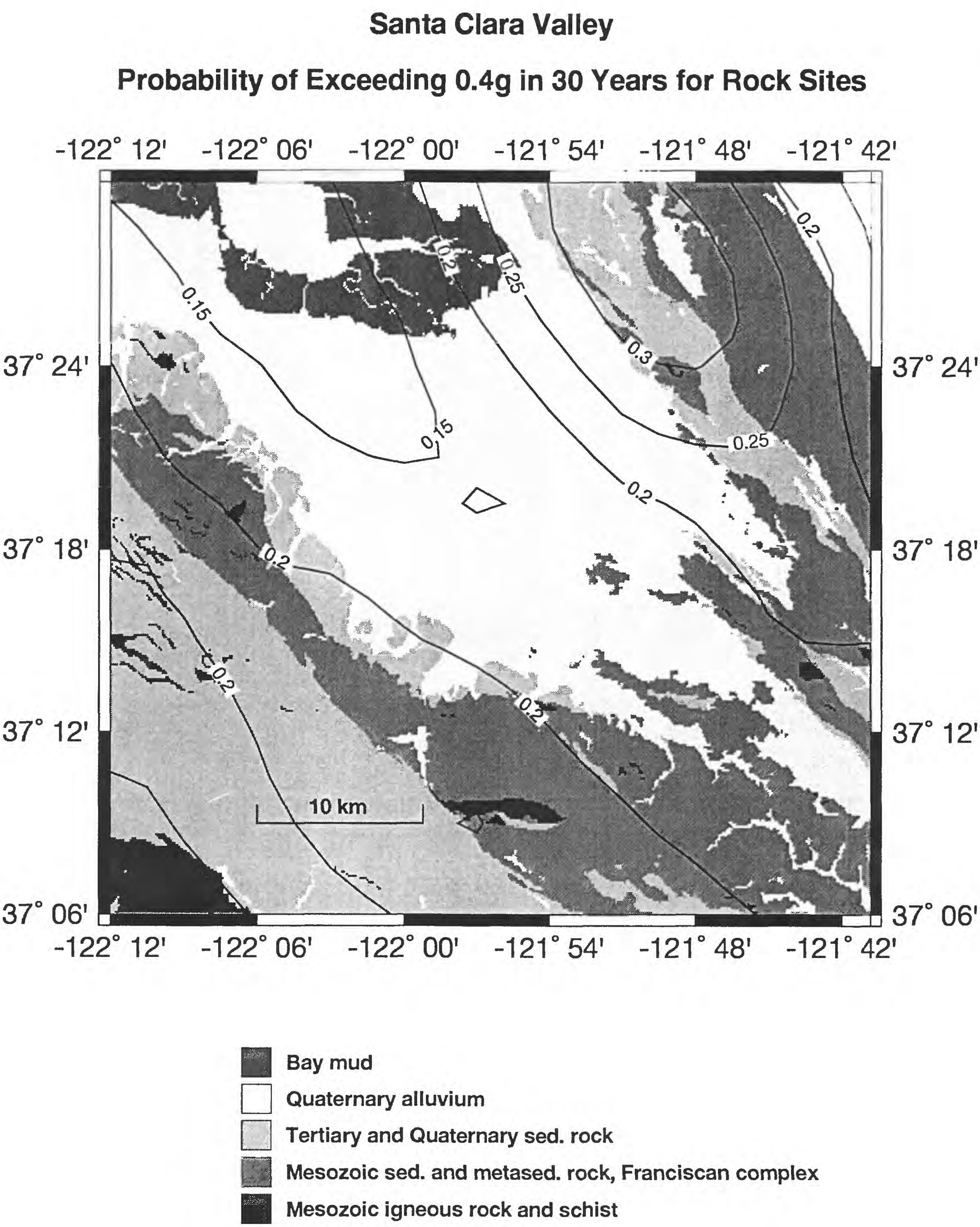
Santa Clara Valley
Probability of Exceeding 0.4g in 30 Years for Rock Sites
-122° 12'
-122° 06'
-122° 00'
-121° 54'
-121° 48'
-121° 42'
37° 24'
37° 18'
37° 12'
37° 06'
0.15
0.2
0.25
0.3
10 km
Bay mud
Quaternary alluvium
Tertiary and Quaternary sed. rock
Mesozoic sed. and metased. rock, Franciscan complex
Mesozoic igneous rock and schist

Figure 1

San Bernardino Valley

Probability of Exceeding 0.4g in 30 Years for Rock Sites

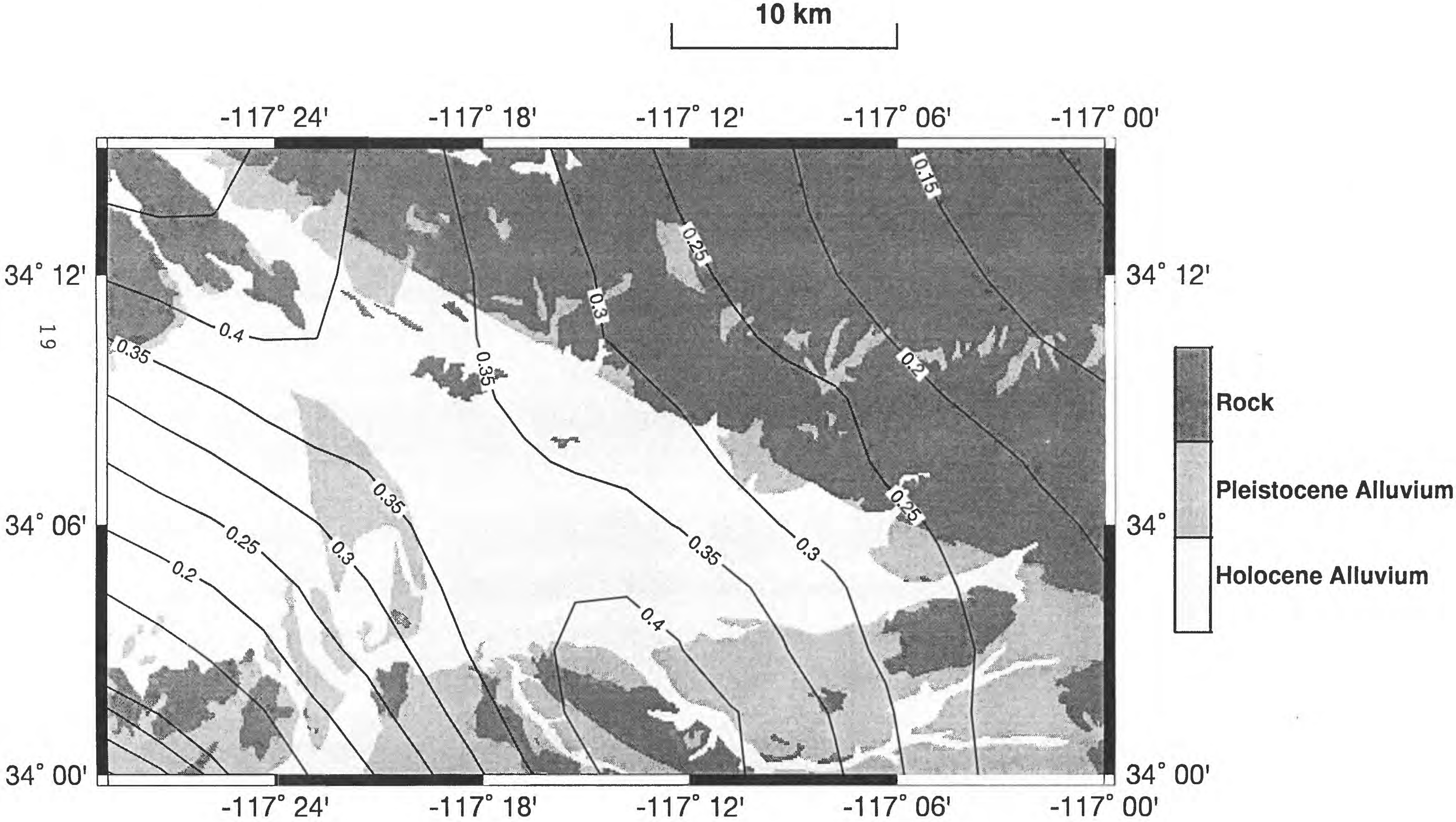

Figure 2

Santa Clara Valley Region
Water Wells

Figure 3

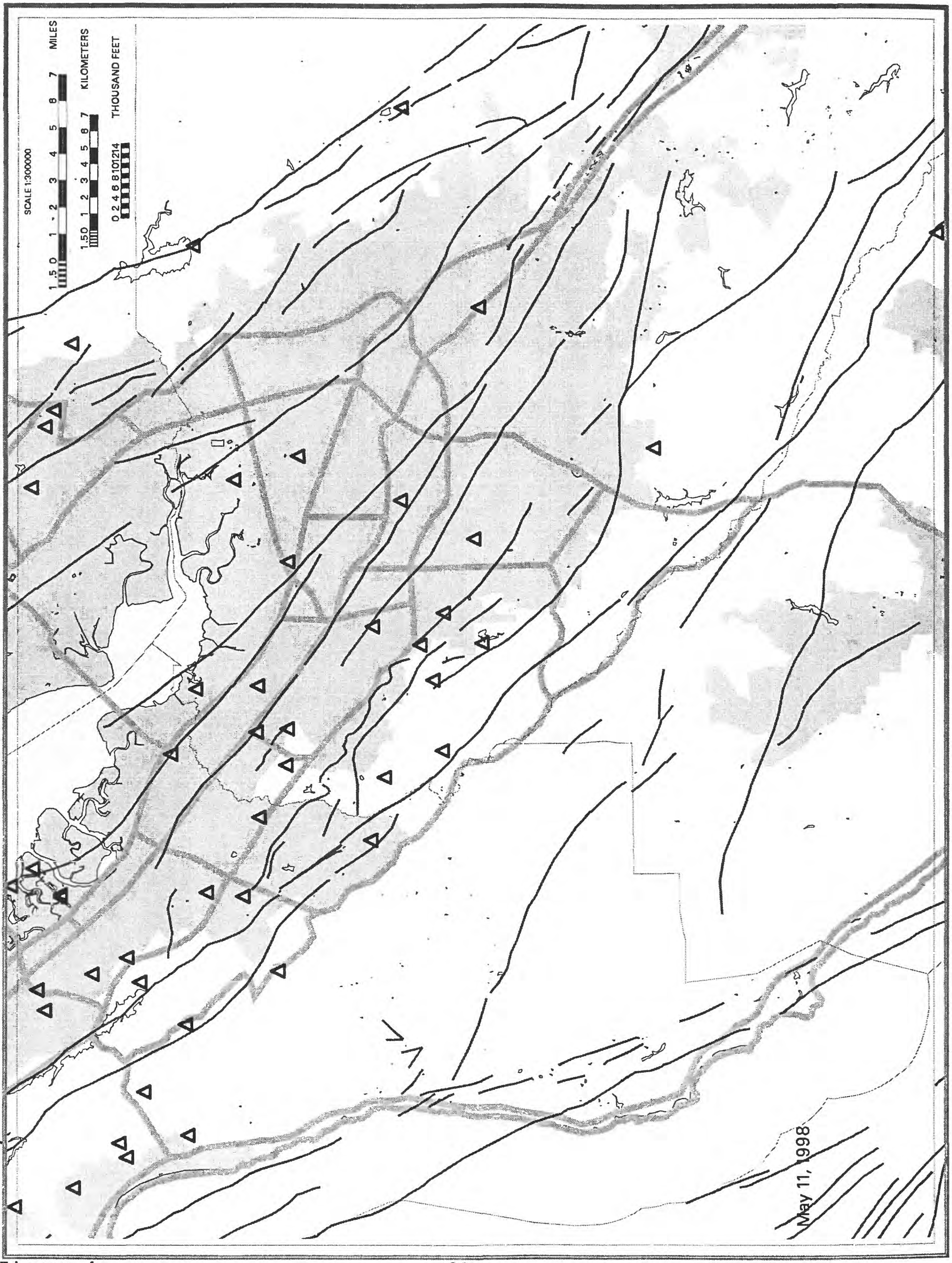

Santa Clara Valley Region
Velocity data

Figure 4

Santa Clara Valley Region
Shot Points and Recievers

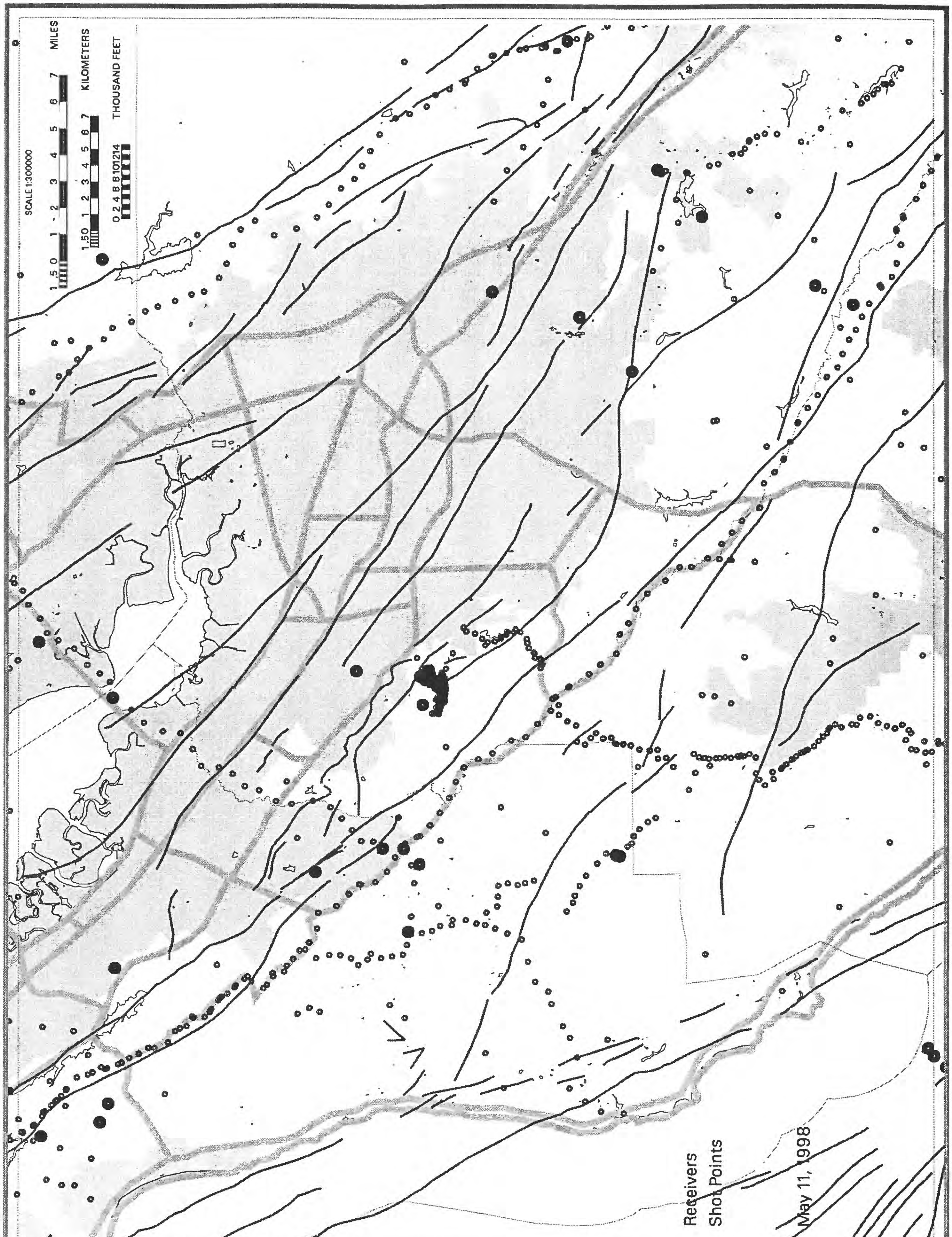

Figure 5

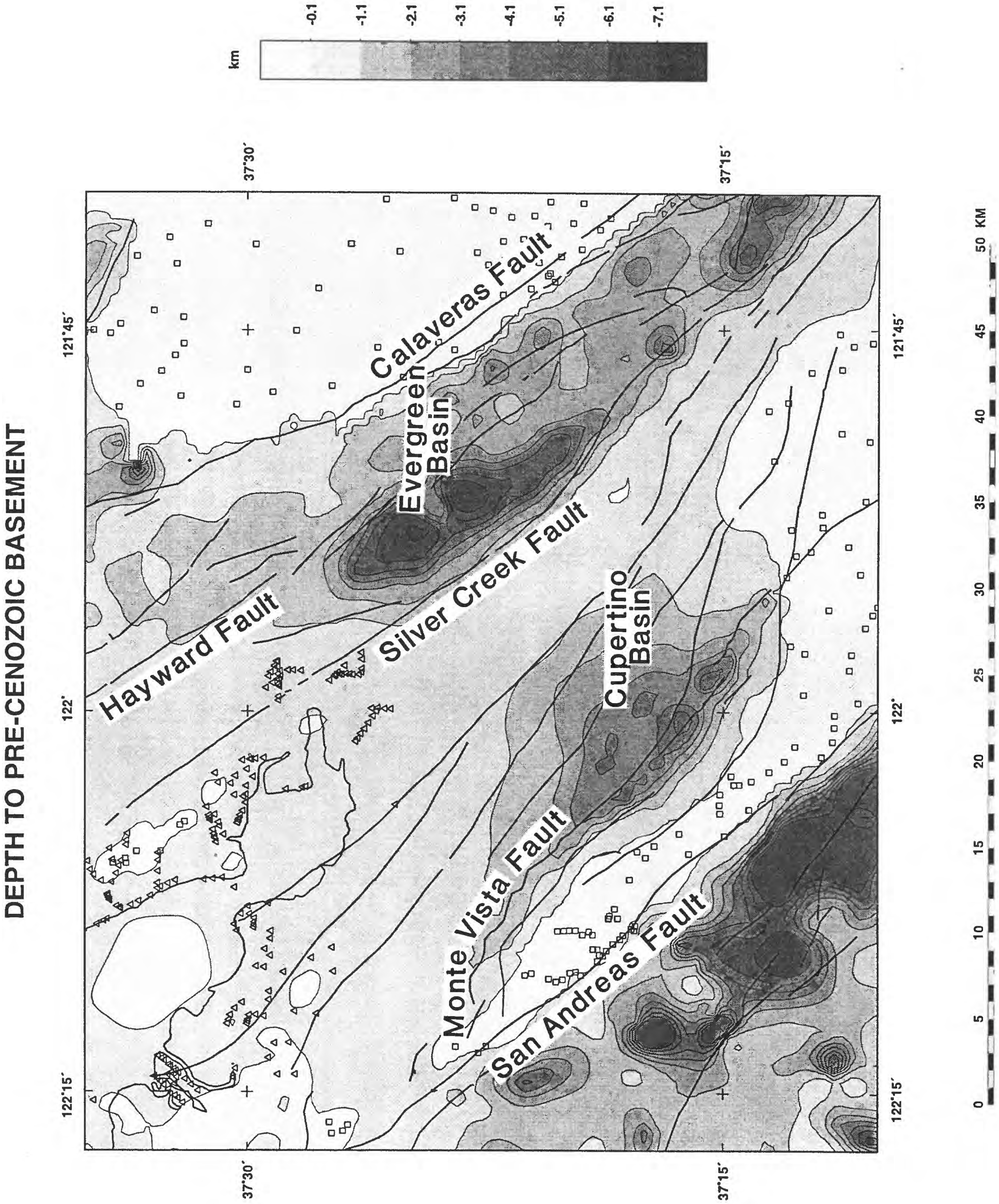
DEPTH TO PRE-CENOZOIC BASEMENT
km
-0.1
-1.1
-2.1
-3.1
-4.1
-5.1
-6.1
-7.1
Calaveras Fault
Evergreen Basin
Hayward Fault
Silver Creek Fault
Cupertino Basin
Monte Vista Fault
San Andreas Fault
37°30'
37°15'
122°15'
122°
121°45'
0
5
10
15
20
25
30
35
40
45
50 KM

Figure 6

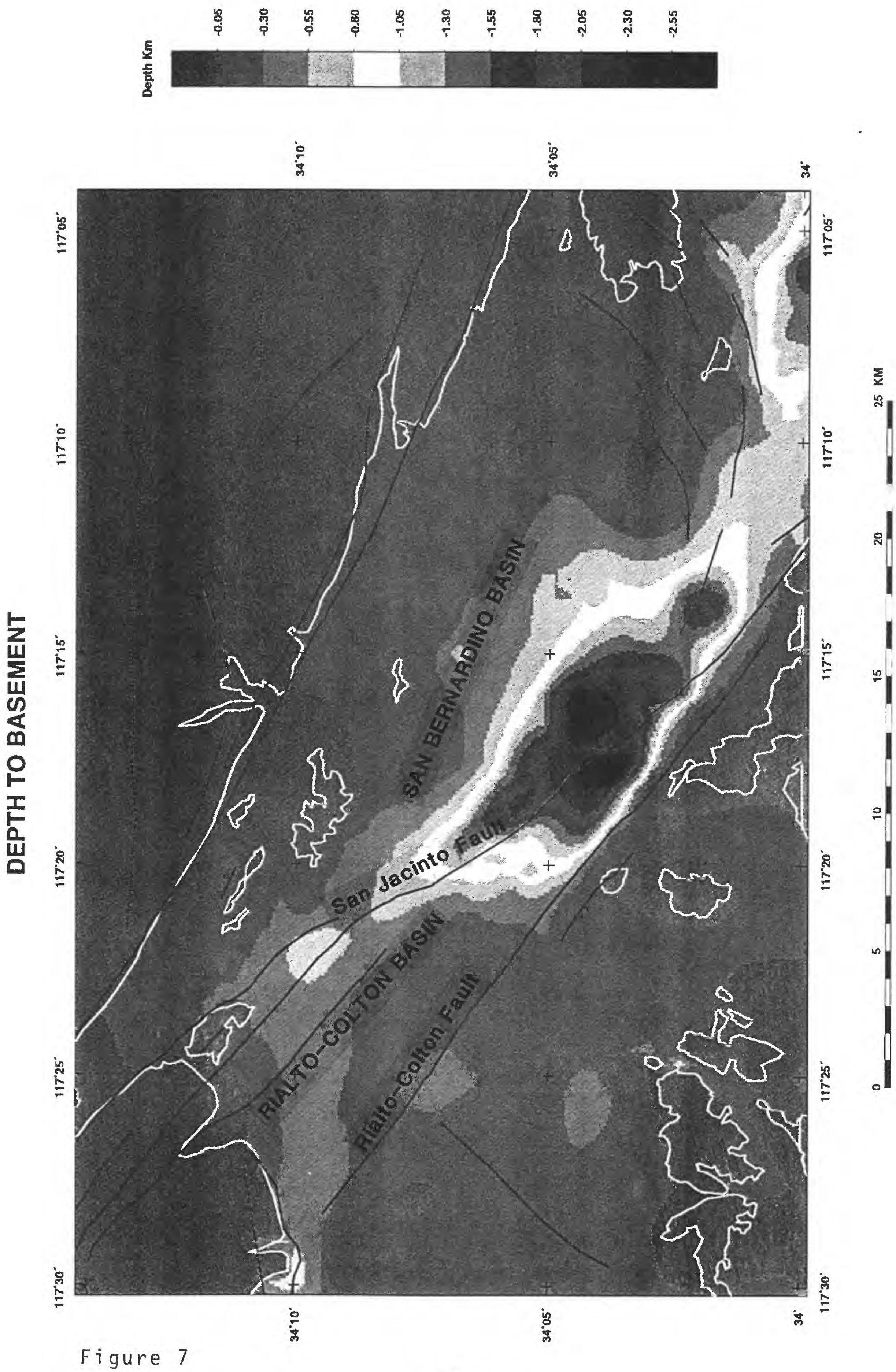
DEPTH TO BASEMENT
Depth Km
-0.05
-0.30
-0.55
-0.80
-1.05
-1.30
-1.55
-1.80
-2.05
-2.30
-2.55
SAN BERNARDINO BASIN
San Jacinto Fault
RIALTO-COLTON BASIN
Rialto-Colton Fault
117°30'
117°25'
117°20'
117°15'
117°10'
117°05'
34°10'
34°05'
34°
0
5
10
15
20
25 KM

Figure 7

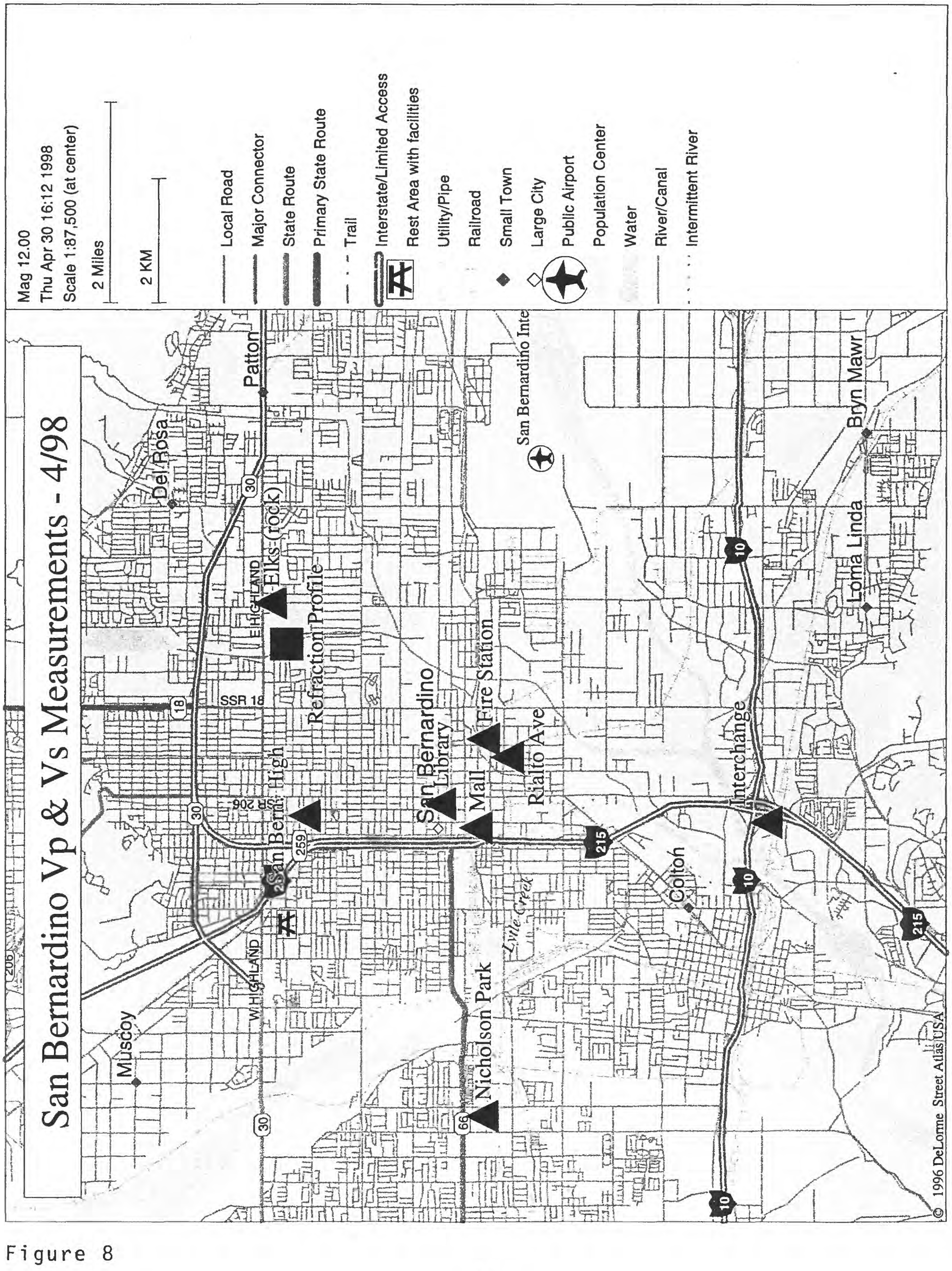
San Bernardino Vp & Vs Measurements - 4/98
Mag 12.00
Thu Apr 30 16:12 1998
Scale 1:87,500 (at center)
2 Miles
2 KM
Local Road
Major Connector
State Route
Primary State Route
Trail
Interstate/Limited Access
Rest Area with facilities
Utility/Pipe
Railroad
Small Town
Large City
Public Airport
Population Center
Water
River/Canal
Intermittent River
Muscoy
Del Rosa
Patton
Elks (rock)
Refraction Profile
San Bernd. High
San Bernardino Library
Mall
Fire Station
Rialto Ave
Nicholson Park
Interchange
Colton
Loma Linda
Bryn Mawr
San Bernardino Inte
Lytle Creek
E HIGHLAND
W HIGHLAND
SSR 18
SR 206
© 1996 DeLorme Street Atlas USA

Figure 8

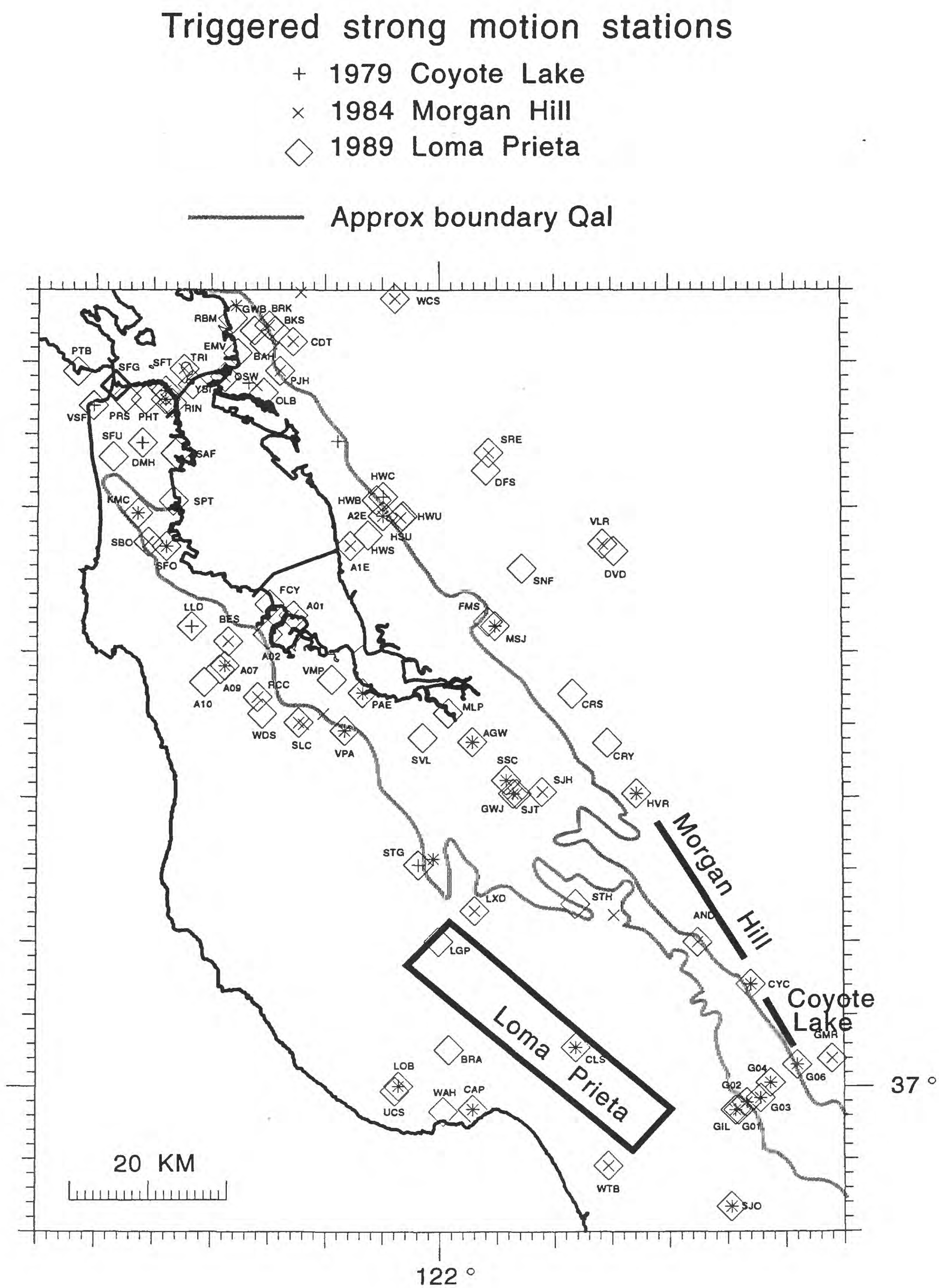

List of triggered stations may be incomplete

Not all triggered stations were digitized

Stations triggered in 1980 Livermore events not shown

Figure 9

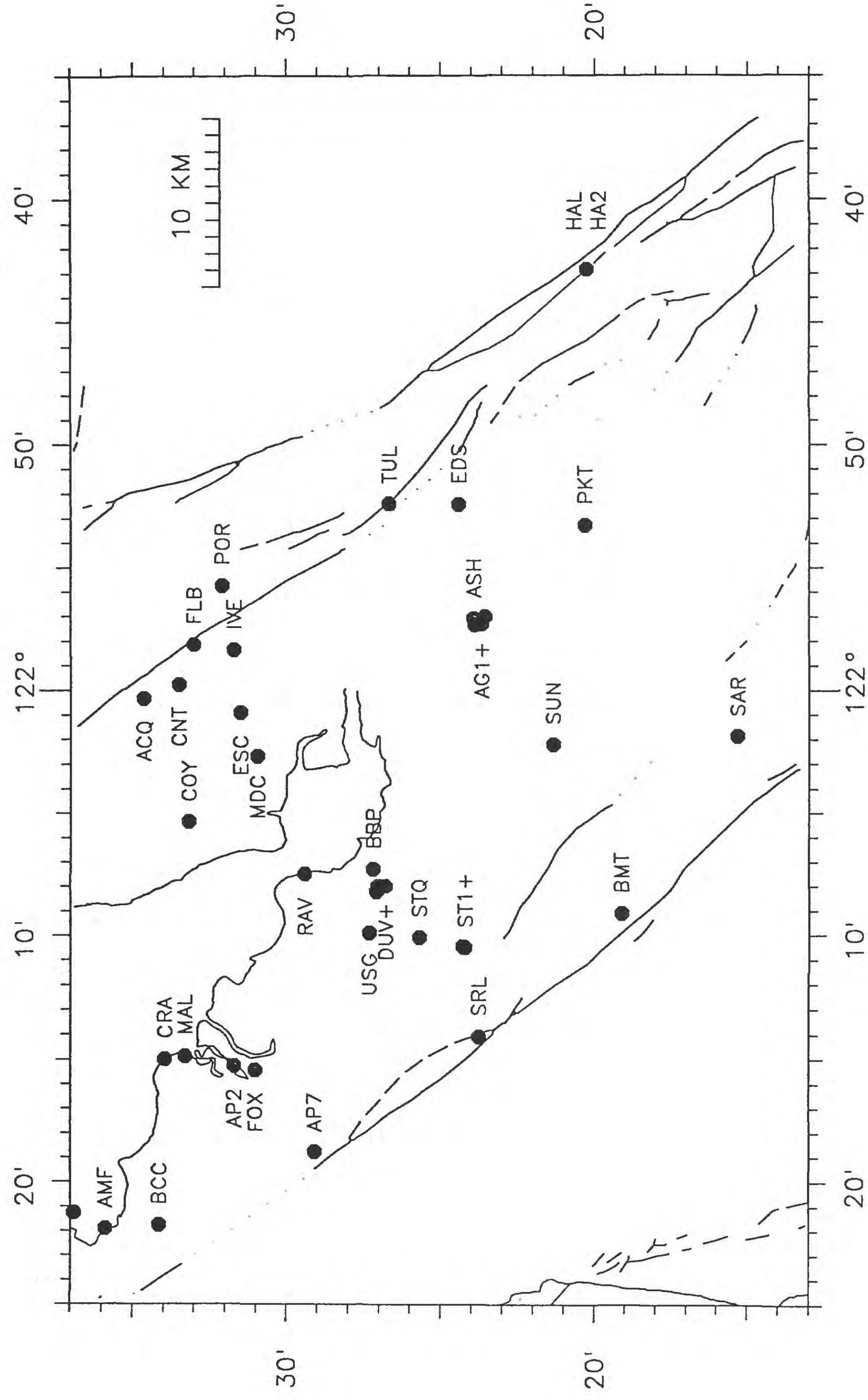
10 KM
40'
50'
122°
10'
20'
30'
ACQ
CNT
COY
ESC
MDC
FLB
IVE
POR
TUL
EDS
PKT
ASH
AG1+
SUN
SAR
HAL
HA2
BRP
RAV
USG
DUV+
STQ
ST1+
BMT
SRL
CRA
MAL
AP2
FOX
AP7
AMF
BCC

Figure 10

Figure 11

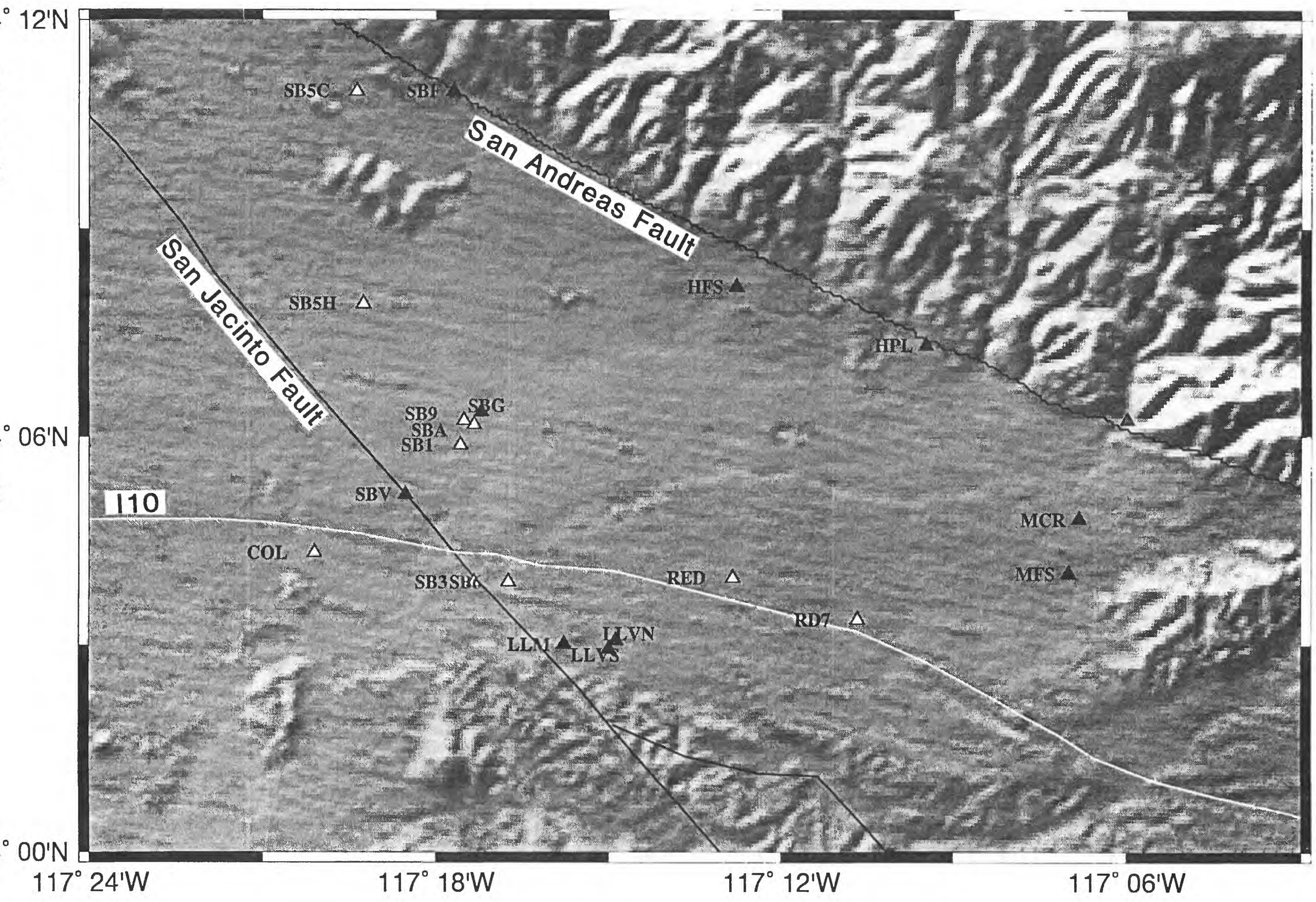

34° 12'N
34° 06'N
34° 00'N
117° 24'W
117° 18'W
117° 12'W
117° 06'W
San Andreas Fault
San Jacinto Fault
I10
SB5C
SBF
HFS
SB5H
HPL
SB9
SBG
SBA
SB1
SBV
MCR
COL
SB3SB6
RED
MFS
RD7
LLVN
LLM
LLVS